Development of ceria-based catalysts for safety production and storage of hydrogen

Tanya Tsoncheva
Institute of Organic Chemistry with Centre of Phytochemistry, Bulgarian Academy of Sciences, Sofia, Bulgaria
Tanya.Tsoncheva@orgchm.bas.bg

Abstract: *This study is aimed at the development of active and selective ceria-based catalysts for hydrogen production by methanol decomposition. The effectc of ceria modification with different metal oxides and development of mesoporous texture of the composites wepe illustrated. The microstructure of the obtained catalysts was studied in details by different physicochemical techniques, such as nitrogen physisorption, XRD, HRTEM, SEM, various spectroscopic methods and TPR with hydrogen. The bi-metallic spinel oxides revealed promising potential for the synthesis of more active and selective catalysts. The catalyst formula was optimized using mesoporous ceria doped with iron oxide as catalyst support and deposition of nickel oxide nanoparticles on it.*

Keywords*: HYDROGEN PRODUCTION; CERIA-BASED CATALYSTS; METHANOL DECOMPOSITION*

1. Introduction

The high energy vector of hydrogen and the practically zero carbon target during the application identify hydrogen as promising alternative fuel in the near future [1,2]. However, the development of the hydrogen-based economy requires fast and efficient solving of the problems related to the low-cost and safety production and storage of hydrogen, without significant changes of the existing infrastructure, especially in case of the mobile and portative installations. Liquid organic compounds could be appropriate hydrogen carrier if they are abundant and cheap enough and also possess sufficient H/C balance. Methanol has been considered as one of the most suitable candidates, even more, it could be produced from diverse sources, including biomass and every waste which could be converted to syngas [3,4].

Among the various technologies for reverse hydrogen release from methanol, the catalytic methanol decomposition seems to be most effective because of easy operation and possibility for energy saving [5,6]. A crucial point of this technology is the efficiency of the catalysts. The intensive study in this aspect reveals that the behavior of the catalysts could be improved if they are produced in nanoscale and by development of porous texture, which ensure high active surface area. The optimization of the bi-functional acid-base and redox properties of the catalysts and the initialization of a synergistic activity between the distinct components in them is also needed. Ceria is one of the most promising candidates of catalyst or catalyst support because it possesses high surface acidity and significant oxygen storage capacity, related to the easy reversible Ce^{3+}-Ce^{4+} transitions [7,8]. It has been reported that the catalytic properties of ceria could be improved via development of mesoporous texture, using hydrothermal preparation procedure in presence of appropriate organic template, and/or by doping it with metal oxides [9,10].

This study is focused at the evolution of ceria - based catalysts for methanol decomposition by modification of ceria with diverse mono-and binary metal oxides. The samples were characterized in details by different physicochemical techniques, such as nitrogen-physisorption, XRD, SEM, HRTEM, various spectroscopic analyses and temperature-programmed reduction with hydrogen. The relation between the microstructure and the optimal formula of the catalysts was clarified as well.

2. Materials and Methods

2.1. Materials

Nanosized mesoporous ceria was synthesized by template assisted hydrothermal technique using aqueous solutions of $CeCl_4$ as a precursor and N- hexadecyl- N, N, N-trimethyl ammonium bromide (CTAB) as a template according to the procedure described in [11]. After the precipitation of the obtained mixture with 25% solution of ammonia, the sludge was subjected to treatment at 373 K for 24 h in a closed container. The produced solid was calcined at 773 K for 10 h in air.

Aqueous solutions of copper, chromium, iron, zinc and nickel nitrates were used for the modification of thus prepared ceria support by incipient wetness impregnation technique. After drying at room temperature, the solid product was subjected to calcination at 773 K for 4 h. For all modifications, the overall amount of metal was 8 wt.%. The monometallic materials were denoted as MCe (M=Cu, Fe, Cr or Ni). For the preparation of binary spinel oxide modifications of ceria, the Cu/Cr and Cr/Fe molar ratio was fixed as 1:2 and the obtained samples were denoted as CuCrCe and FeCrCe, respectively. The ratio between the metals in the ternary CuZnFeCe modification was Cu:Zn=1 and (Cu+Zn)/Fe=1:2, respectively. Alternatively, bi-metallic 1Fe9Ce and 5Fe5Ce mesoporous oxides with Fe/Ce molar ratio of 1:9 and 5:5, respectively, were obtained by hydrothermal technique, following the procedure, reported in [11]. The corresponding Ni5Fe5Fe modification was obtained by incipient wetness impregnation technique, as described above. The Ni content in it was 8 wt.%.

2.2. Methods

Nitrogen physisorption measurements were performed on a Beckman Coulter SA 3100 apparatus. A Bruker D8 Advance diffractometer with Cu Kα radiation and a LynxEye detector with constant step of 0.02° 2θ and counting time of 17.5 s per step was applied for the powder X-ray diffraction analyses. The SEM investigation was carried out on a FEI Nova NanoSEM450. A FEI Talos F200X transmission electron microscope was applied for the HRTEM analyses. UV–Vis measurements were done on a Jasco V-650 UV-Vis spectrophotometer. Raman spectra were collected on a DXR Raman microscope (Thermo Fischer Scientific, Inc., Waltham, MA) equipped with 532 nm laser. The XPS measurements were carried out on a AXIS Supra electron spectrometer (Kratos Analytical Ltd.) using monochromatic AlKα radiation with a photon energy of 1486.6 eV. The Mössbauer spectra at room temperature (RT) were recorded by Wissel (Wissenschaftliche Elektronik GmbH, Germany) electromechanical spectrometer working in a constant acceleration mode. A 57Co/Rh (activity ≈ 10 mCi) source and α Fe standard were used. The spectra were fitted using CONFIT2000 software.

The TPR/TG (temperature-programmed reduction/thermo-gravimetric) analyses were performed on a Setaram TG92 instrument in a flow of 50% H_2 in Ar with heating rate of 5 $K.min^{-1}$.

2.3. Catalytic tests

The catalytic tests were carried out in a flow type fixed-bed reactor (55 mg of catalyst). Methanol (1.57 kPa) was introduced into the reactor from a saturator, thermo-stated at 273 K using argon as a carrier gas (50 $cm^3.min^{-1}$). Step-wise increase of the temperature in the reactor was done up to 773 K keeping the heating rate of 2K/min.

On-line gas chromatographic analyses were performed on a SCION 456-GC apparatus equipped with flame ionization and thermoconductivity detectors using PORAPAC-Q column.

3. Results and Discussion

2.1. Monometallic ceria promoted composites

The texture of the parent ceria and its monometallic modifications was studied by low-temperature nitrogen physisorption. The physisorption isotherms (Fig. 1) characterize with a hysteresis loop between 0.7-0.9 relative pressure and strong increase of the adsorption above it, which is typical of materials with interparticle meso-macroporous texture.

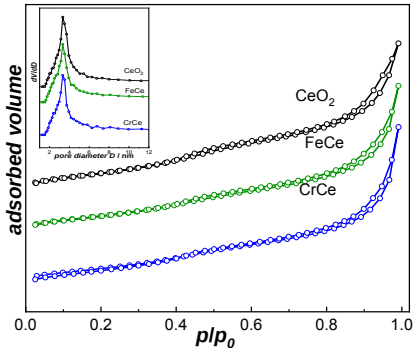

Fig. 1 *Nitrogen physisorption isotherms and pore size distribution (inset) for selected samples.*

The parent ceria possesses about 100 m^2g^{-1} surface area and 0.2 cm^3g^{-1} total pore volume. These parameters decrease of about 10-20% during its modification with different metal oxides. The preservation of the shape of the physisorption isotherms for all modifications (Fig. 1) indicates that the observed effects are predominantly related to partial pore blocking due to the deposition of metal oxide nanoparticles in the pores of the ceria support, without significant structural collapse with it.

SEM and HRTEM techniques were used for the visualization of morphology of the obtained composites (Fig. 2).

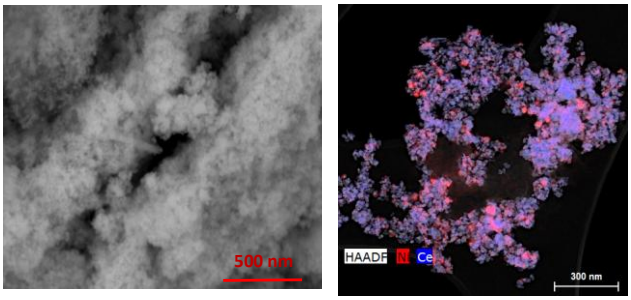

Fig. 2 *SEM (left) and HRTEM (right) images of NiCe composite.*

It was well-illustrated that the ceria matrix possesses garnullar structure of spherical-like nanoparticles. According to the XRD measurements, the average crystallite size was about 11 nm. In the case of the metal oxide modifications, HRTEM images (Fig.2,right) demonstrate presence of metal oxide particles with average size of about 5-10 nm, which are almost homogeneously sprreded within the ceria matrix. This morphology ensures close contact between the ceria support and the loaded metal oxide particles, which could affect the electron transfer between them, initiating sinergistic support-metal oxide activity as well.

Fig. 3a demonstrates methanol decomposition activity of pure ceria and its monocomponent modifications with the temperature increase in the range of 520-770 K. Ceria support exhibits very low catalytic activity. Here, methanol decomposition is initiated just above 700 K and up to 20% selectivity to CO, due to the formation of methane and CO_2 as by-products, is detected (Fig.3b). The shift of the conversion curves to lower temperatures for the metal-modified materials indicates improvement of the catalytic activity (Fig. 3a). CO selectivity increase is also demonstrated in this case (Fig. 3b).

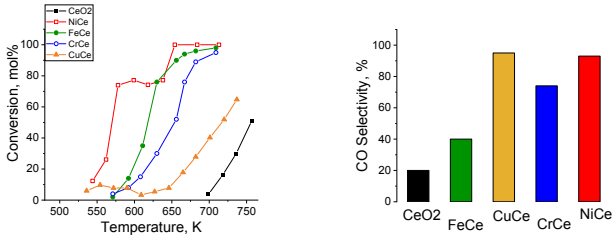

Fig. 3 *Methanol conversion vs temperature (left) and CO selectivity (right) for the monocomponent CeO_2 modifications.*

The modification of ceria with copper is less effective with respect to the development of active catalysts, despite the improved CO selectivity. Just the opposite, significantly higher catalytic activity and lower selectivity in methanol decomposition to CO is demonstrated for the iron- and chromium containing samples. Excellent catalytic behavior, even at relatively low temperatures, is observed for NiCe. However, the complex shape of the conversion curve with the temperature increase indicates significant changes with the catalyst. The additional TPR-TG study clearly demonstrates reduction transformations of the active NiO particles by the reaction medium.

2.2. Spinel oxide ceria promoted composites

In order to improve the behaviour of the Cu and Fe-containing catalyst, binary metal oxide modifications were also produced. Cr was added as a second metal, due to the possibility to obtain binary CuCr and FeCr metal oxides with spinel structure. The superior magnetic, optic and catalytic properties of the spinel materials have been well-demonstrated [12]. They are probably related to their unequal structure, consisted of metal and oxygen ions, arranged with different symmetry in two sub-lattices.

The samples were studied under the conditions of thermo-programmed reduction (TPR) with hydrogen (Fig. 4).

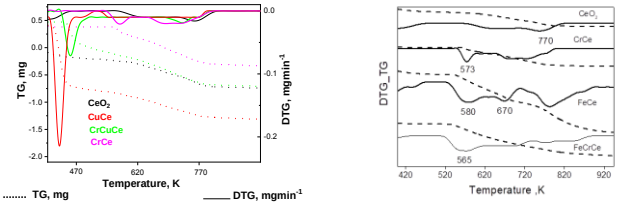

Fig. 4 *TPR-TG and TPR-DTG profiles for CuCrCe (left) and FeCrCe (right) composites. For comparison, monocomponent Fe, Cu and Cr modifications of ceria are also presented.*

The TPR profiles of the individual Cu, Cr and Fe-containing samples significantly change after their combination in the binary materials. This evidences strong interaction between the distinct oxide components, most probably included in the spinel structure.

In order to characterize the changes with the iron components in the binary materials, Moessbauer spectroscopy was also applied. The Moessbauer parameters: isomer shift (IS), quadruple splitting (QS), hyperfine field (H_{eff}) and full width of half-maxima (FWHM) as well as the relative part of each component (G), elucidated by the least squares fitting of a set of discrete Lorentzian line shapes, are listed in Table 1.

The Moessbauer spectra of the mono-component FeCe is well fitted with sextet and doublet parts. The Moessbauer parameters of the sextets (Sx) are typical of Fe_2O_3 with average crystallite size above 10-12 nm. The parameters of the doublet part correspond to Fe^{3+} ions from the "core" and the "shell" of finely dispersed (bellow 10-12 nm) particles with superparamagnetic behavior (SPM).

Doping FeCe with Cr provides disappearance of the sextets in the spectra. The core/shell ratio of the doublets is close to 1, which indicates significant increase in the iron dispersion.

Table 1. *Moessbauer parameters of FeCe and FeCrCe materials*

Sample	Components	IS, mm/s	QS, mm/s	H_{eff}, T	FWHM, mm/s	G, %
FeCe	Sx - Fe^{3+}, γ-Fe_2O_3 Db1 - Fe^{3+}, SPM Fe_2O_3 core	0.34	0.00	49.8	0.64	47
	Db2 - Fe^{3+}, SPM Fe_2O_3 shell	0.36	1.15	-	0.51	26
FeCrCe	Db1 - Fe^{3+}, SPM Fe_2O_3 core	0.35	0.73	-	0.56	46
	Db2 - Fe^{3+}, SPM Fe_2O_3 shell	0.37	1.17	-	0.52	54

The increase in the FWHM values for FeCrCe evidences change in the environment of the iron ions, most probably due to the interaction with the situated nearby chromium ions.

In Fig.5 the catalytic behavior of all mono- and bi-component Cu, Cr and Fe containing samples in methanol decomposition is compared.

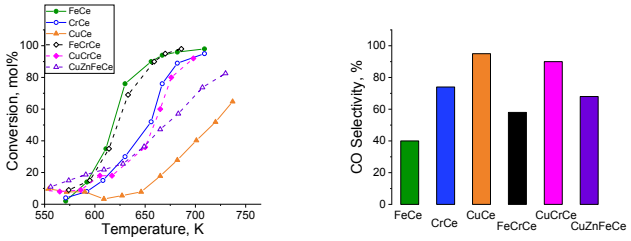

Fig. 5 *Methanol conversion vs temperature (left) and CO selectivity (right) for the mono- and bi-componnet Cu and Fe modifications of CeO_2.*

The methanol conversion is strongly improved for the CuCrCe composites with respect to the corresponding ingredients, without significant changes in the CO selectivity. The catalytic activity of FeCrCe is similar to that one of FeCe, despite the lower content of iron in the former. Here, simultaneous increase of the CO selectivity is also detected. Considering the Moessbauer results (Table 1), these observations could be related to the stabilization of iron and copper species in highly dispersed state. Their catalytic behaviour is also affected by the easier reduction transformations of the iron and suppressed reduction transitions in the copper species under the reduction reaction medium (Fig.4).

The evolution of the Cu- and Fe-ceria modifications after doping with zinc oxide, was followed in the obtained ternary CuZnFeCe composites. The XRD results show co-existence of cerianite and ferrite phases with average crystallite size of 22 and 16 nm, respectively. The TEM images (Fig.6, left) demonstrate high dispersion and close contact between the distinct metal oxide species.

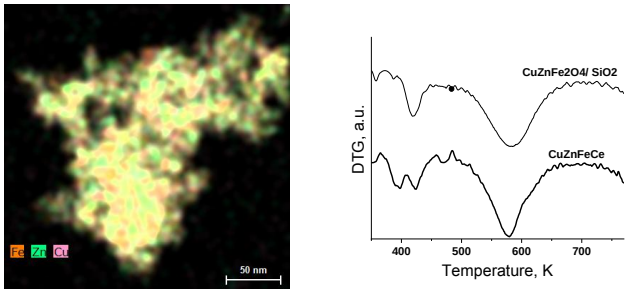

Fig. 6 *TEM image of CuZnFeCe composite (left) and TPR of CeO_2 and SiO_2.supported CuZnFe (right).*

The TPR profiles (Fig. 6, right) show reduction transformations with the ferrite phase in the 400-650 K range. Note, that the TPR effects of CuZnFeCe are narrower and shifted to lower temperature in comparison with the similar CuZnFe modification of the inert silica support. This suggests complex influence of the ceria support on the loaded spinel particles, which probably improves not only their dispersion, but also the electron transfer from the support to the loaded spinel oxide particles.

The ternary CuZnFeCe composite demonstrates higher catalytic activity, but about 25% lower CO selectivity as compared to the single CuCe modification (Fig.5). In comparison with FeCe, the CuZnFeCe sample possesses much lower catalytic activity, but about double higher CO selectivity.

Thus, the spinel oxides provide good oportunity for the improvement of the ceria catalytic behaviour in methanol decomposition and the catalyst formula could be optimized by simple varriation of the spinel oxide composition.

2.3. Nickel and iron ceria promoted composites: Effect of the preparation procedure.

The preparation procedure is a powerful strategy for the regulation of catalyst behavior. In this study, FeCe and 1Fe9Ce materials with similar Fe content were prepared by traditional incipient wetness impregnation and template assisted hydrothermal technique, respectively. The XRD study (Table 2) demonstrates higher dispersion of the samples, prepared by the addition of iron during the hydrothermal treatment. For this sample, a slightly higher BET surface area and pore volume is registered (Table 2), which evidences lower effect of pore blocking. Using similar hydrothermal technique, the 5-fold increase of the iron content in the sample (5Fe5Ce) provides a significant decrease in the BET surface area and pore volume combined with a segregation of hematite phase with average crystallite size of about 42 nm (Table 2). For both 1FeCe and 5Fe5Ce samples a deviation in the ceria unit cell parameters is observed which indicates that the hydrothermal procedure facilitates partial insertion of Fe^{3+} ions in the ceria lattice.

Table 2. *XRD and N_2 physisorption data for Fe and Ni decorated CeO_2.*

Sample	Phase composition	Unit cell parameters (Å)	Crystallite size, nm	BET, m^2/g	Pore volume, m^3/g
CeO_2	CeO_2	5.4126(5)	18	105	0.22
FeCe	CeO_2	5.4126(5)	18	90	0.19
1Fe9Ce	CeO_2	5.3948(8)	11	99	0.25
5Fe5Ce	CeO_2 Fe_2O_3	5.374(1) a=5.044(1) c=13.78(4)	8 42(3)	68	0.37
NiCe	CeO_2 NiO	5.4119(4) 4.184(1)	19(18) 15	41	0.16
Ni5Fe5Ce	CeO_2 Fe_2O_3 NiO	5.375(1) 5.046(1) 13.781(4) 4.190(3)	9(8) 48(42) 13	58	0.27

The modification of ceria with Ni and Fe provides significant change in the optical properties, which is well-illustrated by the changes in the absorption features in the UV-Vis spectra (Fig. 7).

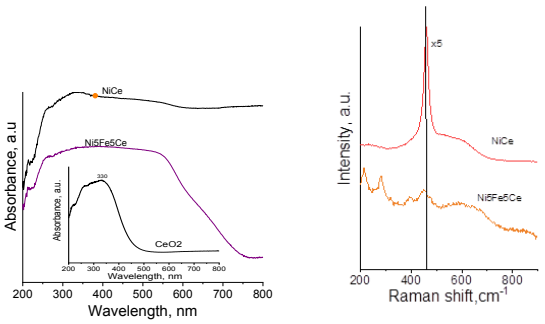

Fig. 7 *UV-Vis (left) and Raman (right) spectra of NiCe and Ni5Fe5Ce composites.*

This could be assigned to significant changes in the environment of the cerium ions due to the situated nearby Fe^{3+} and

Ni^{2+} ions and related with them, oxygen deffects. The Raman specta (Fig.7) display strong decrease in the intesity of the typical of ceria Raman shifts, especially in case of the Fe-doped materials. This indicates changing in the ceria microstructure due to the incorporation of Fe^{3+} and/or Ni^{2+} ions in it.

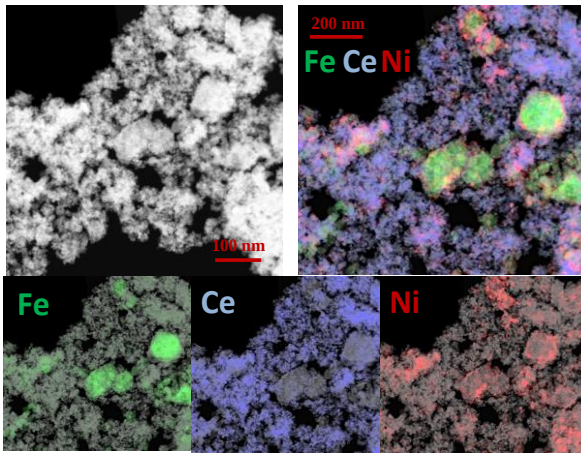

Fig. 8 *TEM image of Ni5Fe5Ce composite.*

TEM images of Ni5Fe5Ce is presented in Fig. 8. It is well visible that the Fe particles are finely dispersed within the whole CeO_2 matrix. Only small number of larger Fe-containing aggregates could be distinguished, which is in accordance with the XRD study (see above). The Ni-containing particles, which are also with very high dispersity, seems to be in close contact both with ceria and iron-containing species.

More information for the surface distribution of all elements in various composites was obtained by XPS technique (Table 3).

Table 3. *Data from the XPS analyses for the selected Ni and Fe decorated CeO_2.*

Samples	O 1s, at %	Fe 3p, at %	Ni 3p, at %	Ce 3d, at %	Ce^{3+} %
CeO2	79.5	-	-	20.5	22.6
NiCe	80.8	0.0	6.5	12.7	8.0
1Fe9Ce	59.4	8.2	-	32.4	34.3
5Fe5Ce	63.1	11.7	-	25.2	27.7
Ni5Fe5Ce	77.0	4.5	3.1	15.4	15.0

Co-existence of Fe^{3+}, Ni^{2+}, Ce^{4+} and Ce^{3+}- containing phases is detected. The presence of significant amount of cerium in lower oxidative state evidences formation of defects in the ceria lattice, most probably related to the replacement of Ce^{4+} ions by Fe^{3+} and /or Ni^{2+} ones. This ensures higher concentration of the latter on the surface as compared to the expected nominal ones. Note, that the Ni/Fe ratio is about 1.5, which is close to the theoretic ratio in the Ni ferrite. These results could be an indication for the preferable location of the Ni ions around the Fe-containing species, most probably on the Fe-Ce interface.

The catalytic behavior of the samples is illustrated in Fig. 9. All modifications exhibit higher catalytic activity and CO selectivity as compared to the pure ceria support. Among the mono-component iron modifications, the impregnation technique facilitates the formation of more active, but less selective to CO samples. Obviously, the higher extent of insertion of Fe^{3+} ions in the ceria matrix, which is achieved by the hydrothermal preparation technique, forms lower number, but highly active in methanol dehydrogenation to CO catalytic sites. The segregation of larger hematite particles, which is facilitated with the increase in the Fe/Ce ratio (sample 5Fe5Ce), improves the catalytic activity, but decreases the selectivity to CO.

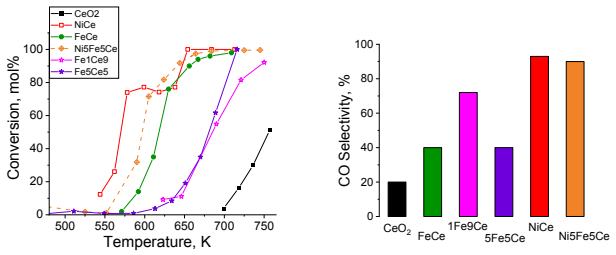

Fig. 9 *Methanol conversion and CO selectivity for Ni and Fe-decorated CeO_2.*

As demonstrated above, NiCe modification demonstrates superior catalytic activity and CO selectivity at lower temperatures, but the catalyst significantly loses its activity above 570 K, most probably due to the reduction and segregation of the actve Ni-species by the influence of the reaction medium. This disadvantage is overcome by Fe-doping of ceria during the hydrothermal procedure (sample Ni5Fe5Ce). It seems that the localization of Ni^{2+} ions in the vicinity of the Ce/Fe interface stabilizes them in highly dispersed state and probably provokes the activity of mixed Ni-Fe-Ce redox pairs.

4. Conclusions

The catalytic activity and selectivity of mesoporous CeO_2, prepared by template assisted hydrothermal technique, in methanol decomposition could be significantly increased after modification with Cu, Fe, Ni or Cr oxides by simple incipient wetness impregnation procedure. The catalytic behaviour of these composites could be improved by development of binary oxides with a spinel structure. The Ni modification of ceria provides superior catalytic activity in selective decomposition of methanol to CO and the catalyst stability could be improved by preliminary doping of ceria with iron oxide using hydrothermal prepation procedure.

Financial support

Project BG05M2OP001-1.002-0019„Clean technologies for sustainable environment–water, waste, energy for circular economy“ (Clean&Circle) and Bulgarian Scientific Fund, Grant KP06H 29/2.

References

1. K. Mazloomi, C. Gomes, Renew. Sust. Energy Rev. 16, 3024 (2012).
2. M. Granovskii, I. Dincer, M. A. Rosen, Int. J. Hydrogen Energy. 31, 337 (2006).
3. J. Andersson, A. Krüger, S. Grönkvist, Energy Conv. Manag. X 7 100051 (2020).
4. S. Bepari, D. Kuila, Int. J. Hydrogen Energy 45, 18090 (2020).
5. S. Qing, X. Hou, L. Li, G. Feng, X. Wang, Z. Gao, W. Fan, Int. J. Hydrogen Energy 44, 16667 (2019).
6. G. A. Olah, Catal. Lett. 93, 1 (2004).
7. A. Trovarelli. Catal, Rev. Sci. Eng. 38, 439 (1996).
8. N. Laosiripojana, S. Assabumrungrat, Chem. Eng. Sci. 61, 2540 (2006).
9. L. P. Matte, A. S. Kilian, L. Luza, M. C. M. Alves, J. Morais, D. L. Baptista, J. Dupont, F. Bernardi. J. Phys. Chem. C 119, 26459 (2015).
10. X. Zhu, M. Zhang, K. Li, Y. Wei, Y. Zheng, J. Hub, H. Wang, Chem. Eng. Sci. 179, 92 (2018).
11. T. Tsoncheva, C. Rosmini, M. Dimitrov, G. Issa, J. Henych, Z. Němečková, D. Kovacheva, N. Velinov, G. Atanasova, I. Spassova. ACS Appl. Mater. Interfaces 13, 1838 (2021).
12. B. I. Kharisov, H. V. R. Dias, O. V. Kharissova, Arabian J. Chem. 12, 1234 (2019).